The mRNA content of plasma extracellular vesicles provides a window into the brain during cerebral malaria disease progression

Abdirahman Abdi (AAbdi@kemri-wellcome.org)
KEMRI Wellcome Trust Research Programme https://orcid.org/0000-0001-7989-2125
Kioko Mwikali
KEMRI Wellcome Trust Research Programme
Shaban Mwangi
KEMRI Wellcome Trust Research Programme
Alena Pance
University of Hertfordshire https://orcid.org/0000-0002-9017-2644
Lynette Ochola-Oyier
KEMRI-Wellcome Trust Research Programme
Symon Kariuki
skariuki@kemri-wellcome.org
Charles Newton
cnewton@kemri-wellcome.org
Philip Bejon
KEMRI-Wellcome Trust Research Programme, Centre for Geographic Medicine Research - Coast
Julian Rayner
University of Cambridge https://orcid.org/0000-0002-9835-1014

Article

Keywords:

Posted Date: September 28th, 2023

DOI: https://doi.org/10.21203/rs.3.rs-3375373/v1

Abstract

The impact of cerebral malaria on the transcriptional profiles of cerebral tissue is difficult to study using non-invasive approaches. We isolated plasma extracellular vesicles (EVs) from patients with cerebral malaria and community controls and sequenced their RNA content. Deconvolution of the tissue origins of the EV-RNA revealed that EVs from cerebral malaria patients are predominantly enriched in transcripts of brain origin. Next, we used manifold learning on the EV-RNAseq data to determine pseudotime against the community control samples as the baseline reference. We found that neuronal transcripts in plasma EVs decreased as pseudotime progressed, while transcripts of glial, endothelial, and immune cell origins increased over pseudotime. Pseudotime was associated with clinicopathological parameters of disease severity, including retinopathy, metabolic acidosis, respiratory rate, anaemia, malnutrition, depth of unconsciousness and death. Plasma EVs further provided evidence of platelet activation, TNF signalling, neurotrophin signalling, long-term potentiation and glutamatergic signalling during late disease stages of cerebral malaria. The transcriptional responses of cerebral tissue in cerebral malaria can be studied non-invasively using EVs circulating in peripheral blood.

Introduction

Cerebral malaria is an encephalopathy caused by *Plasmodium falciparum* infection [1,2]. Cerebral malaria was originally defined clinically as a coma in the presence of peripheral blood parasitaemia and not directly attributable to other causes such as hypoglycaemia, convulsion and meningitis [3]. Sequestration of parasitised erythrocytes in the brain microvascular system is a key mechanism leading to neurological impairment and the driver of disease severity in cerebral malaria [2]. However, the cerebral tissues can only be studied directly during postmortem evaluation [4].

This limitation has motivated the search for non-invasive ways of accurately diagnosing cerebral malaria. The retina comprises brain-like tissues and shows parasite sequestration and pathology comparable to that in canonical brain tissues [5–7], but unlike the brain, the retina can be directly visualised; thus, sequestration-associated retinal pathology can be visualised clinically via non-invasive ophthalmological techniques [8]. This approach revealed a retinal pathology, termed "retinopathy", that can be used as a surrogate marker for parasite sequestration in the brain [9–12]. Patients with retinopathy-positive cerebral malaria (CM-R^+) are then considered the "true" cases of *P. falciparum*-induced cerebral pathology [9,13]. In contrast, those with retinopathy-negative cerebral malaria (CM-R^-) are suspected of having either encephalopathy caused by other aetiologies with incidental *P. falciparum* infection [9,13], or coma secondary to systemic disturbance (e.g. metabolic consequences of malaria such as hypoglycaemia). Retinopathy was found to be highly sensitive (87–100%) and specific (75–87%) for cerebral malaria caused by *P. falciparum* [14], but it provides no information on the molecular mechanisms of cerebral malaria pathogenesis.

We propose an alternative non-invasive approach through extracellular vesicles (EVs) circulating in the blood. EVs are nanosized molecules secreted by all cells into biological fluids and are surrounded by a limiting phospholipid membrane [15]. They contain biological cargo such as RNA, lipids, and proteins reflecting the metabolic and physiological status of the parent cells or tissues. EVs can also cross tissue-blood barriers and circulate in biofluids without diluting their contents. This makes EVs attractive non-invasive tools for studying the pathology of diseases affecting inaccessible tissues, such as cerebral tissue [15], in contrast to circulating immune cells that provide information limited to the immune compartment [16,17].

The temporal molecular alterations that occur as cerebral malaria progresses cannot be obtained through time series data from cerebral malaria patients because of the ethical imperative to begin treatment, and patients often present at hospitals at varying stages of disease progression after an unknown period of pre-admission illness. Researchers in other fields have used pseudotime or trajectory inference methods such as manifold learning to construct pseudo-temporal models of disease progression using gene expression data from cross-sectional samples [18,19]. Pseudotime inference algorithms work under the premise that each sample represents a snapshot of a disease stage and that the notional sampling time varies among the patients [20]. Here, we apply pseudotime analysis to construct a cerebral malaria disease progression model based on plasma EV transcriptomes from cross-sectional samples obtained from CM-R^+ and CM-R^- patients using samples from healthy community controls as a baseline reference group.

Results

Solid tissue atlas of plasma-derived EVs in cerebral malaria.

The study included 76 children admitted with cerebral malaria at Kilifi County Hospital (KCH) as previously described [21,22] (clinical parameters provided in **Suppl data 1**) and 8 community controls (CC) without *P. falciparum* infection. We sequenced the RNA content of plasma EVs from all individuals and applied support vector regression [23,24] to deconvolute the composition of solid tissues and brain cells in our EV-RNAseq data (Fig. 1a-d; **Suppl Fig. 1a**). We found that 32.2% of the plasma EV-RNA isolated from cerebral malaria patients originated from genes highly expressed in solid tissues (Fig. 1a), and 67.8% were from genes highly expressed in whole blood cells (Fig. 1a). Within the solid tissue fraction, the brain predominated (37.7%), followed by peripheral nerves (14.4%) and the small intestines (7.7%), (Fig. 1b; **Suppl Fig. 1a**). Additionally, the absolute proportion of RNA from transcripts expressed by the brain and peripheral nerves was relatively higher in CM-R^+ and CM-R^- compared to CC (Fig. 1c). Within the brain fraction, RNA from genes highly expressed in brain-endothelial cells (32%), microglia (27.6%), and neurons (26.2%) dominated the plasma EV-transcriptomes, while genes expressed in other brain cell types contributed less than 10% (Fig. 1d). To validate the EV deconvolution approach, we downloaded and deconvoluted plasma EV-RNAseq data (GSE100207) generated from hepatocellular carcinoma (HCC) patients [25]. We observed that tissue-derived plasma EV-RNA in HCC patients originated predominantly

from the liver (31.9%) and the adipose tissue (23.5%) (**Suppl Fig. 1b-c**), thus validating the EV-origin deconvolution analysis.

Plasma EV-RNA resolves the heterogeneity among cerebral malaria patients and identifies retinopathy as a late-stage disease phenotype.

We explored whether plasma EV transcriptomes reflected the heterogeneity of clinically defined cerebral malaria patients and whether they could be used to resolve disease progression at the molecular level. Applying manifold learning to the EV transcriptomes obtained from the cross-sectionally sampled patients, we defined the molecular disease stage of the samples - often called pseudotime or trajectory [18] (Fig. 2a). The samples from malaria patients were ordered based on their similarity in EV-RNA abundance using the community control (CC) samples as the baseline reference, and this order was used to infer the molecular disease pseudotime (Fig. 2a). Samples with later pseudotime were primarily seen among the CM-R^+ patients while earlier pseudotime samples primarily originated from CM-R^- and CC (Fig. 2a-b). We adopted a statistical approach to compare disease pseudotime between CM-R^+, CM-R^-, and CC and found that disease progression was significantly (p-value < 0.001) more advanced in CM-R^+ compared to CM-R^- (Fig. 2c). Using receiver operating characteristic (ROC) analysis, we benchmarked pseudotime against retinopathy and found retinopathy was 100% sensitive and about 78% specific for late-stage cerebral malaria (Fig. 2d). Next, we applied linear regression to assess whether disease pseudotime was associated with clinicopathological parameters provided in **Suppl data 1**. Later pseudotime was positively associated with retinopathy, metabolic acidosis, in-hospital death, and respiration rate, and negatively associated with mid-upper arm circumference (MUAC; a surrogate for nutritional status), haemoglobin (Hb) and Blantyre Coma Scores (BCS) (Fig. 2e). Surprisingly, measures of parasitaemia (peripheral parasitaemia and *Pf*HRP2) were not associated with disease pseudotime, suggesting that cerebral disease progression was not simply a correlate of parasite burden (Fig. 2e). These observations suggest that pseudotime, as calculated here, is an accurate proxy for disease progression.

Alteration of plasma EV transcriptomes as a function of pseudotime.

We fitted harmonic regression models to the gene profiles and found that 70% of the total EV transcripts (7438/10150) were significantly altered as a function of pseudotime (nominal p-value < 0.05) (**Suppl data 2**). We constructed a phaseogram of disease progression using the significantly altered transcripts, and gene clustering analysis over pseudotime identified four non-overlapping gene clusters, which we named c1 to c4 (Fig. 3a; **Suppl data 2)**. We used Fisher's exact test to analyse the gene overlap between the clusters and reference lists of published cell-type-specific markers [26,27]. Early disease-stage clusters (c1 and c2), which decreased with disease progression, were enriched for neuronal gene sets, while the late ones (c3 and c4), which increased with disease progression, were enriched for glial (astrocytes, and microglia) gene sets (Fig. 3b-c; **Suppl data 3; Suppl data 4**). We exemplify the above observations using smoothed curves of five neuronal markers, including serotonin receptor (HTR5A), glial-derived neurotrophic factor receptor alpha 2 (GFRA2), and ganglioside-induced differentiation-associated protein 1 (GDAP1) and five glial cell markers, the most notable being markers of reactive gliosis, neurocan

(NCAN) [28] and glial fibrillary acidic protein (GFAP) [29], and the astrocytic water channel aquaporin 4 (AQP4) [30] (Fig. 3d). Transcripts belonging to immune cells, notably neutrophils and erythropoiesis (erythroblasts) were enriched in late disease-stage clusters (c3 and c4) (Fig. 3b; **Suppl data 4**). These results insinuate that cerebral malaria proceeds along a smooth transcriptional cascade of declining neuronal transcripts and a progressive increase in glial and immune cell transcripts, which can be studied via EVs circulating in peripheral blood.

Lastly, we performed enrichment analysis using the KEGG gene sets [31] to determine whether transcripts enriched in late pseudotime clusters (c3 and c4) belong to biological pathways that could be associated with cerebral malaria pathogenesis. We found that cluster 3 genes were linked to neural functions (long-term potentiation, glutamatergic synapse and neurotrophin signalling) and vascular processes (TNF signalling, VEGF signalling, platelet activation and the complement cascade), while cluster 4 was enriched for genes implicated in age-related disorders such as Parkinson's disease, amyotrophic lateral sclerosis, Huntington's disease and Alzheimer's diseases (Fig. 3e; **Suppl data 5**). When we performed enrichment analysis using the Wikipathway genesets [32], we noted that "neuroinflammation and glutamatergic signalling" and "VEGFA-VEGFR2 signalling" were associated with late pseudotime clusters (Fig. 3f; **Suppl data 6**). Taken together, our data proves that it is feasible to non-invasively study the pathological processes that drive infectious encephalopathies such as cerebral malaria by analysing the biological contents of circulating EVs.

Discussion

Cerebral malaria is a complication of *P. falciparum* characterised by impaired consciousness, among other neurological complications [1,33]. However, despite extensive research, the pathological process by which malaria parasites cause cerebral malaria[34,35] is poorly defined. In this study, we hypothesised that the RNA content of circulating extracellular vesicles (EVs) could be used to study neuropathological processes during cerebral malaria, specifically the transcriptional profiles of cerebral tissue. We show that the RNA content of circulating EVs reflects biological processes that occur as cerebral malaria progresses and could be used as a non-invasive means to study disease mechanisms and identify diagnostic biomarkers.

Our results showed that after blood, brain cells predominated as the source of circulating EV-RNAs in cerebral malaria patients. Our analysis of pseudotime revealed that retinopathy is a late-stage disease marker. This implies that CM-R^- might be a less severe form of cerebral malaria that can progress to CM-R^+, which is consistent with other recent data[36] and challenges the dogma that CM-R^- represents encephalopathies of other aetiologies besides *P. falciparum* [9,13]. Consistently, pseudotime was also positively associated with other malaria clinicopathological parameters of severity, such as in-hospital death, metabolic acidosis, raised respiratory rate, anaemia, and depth of coma, reinforcing the hypothesis that pseudotime, as a latent variable calculated from the EV-RNAseq data, represents cerebral malaria progression.

We observed declining neuronal transcript levels during the late-disease stage, which coincides with increased glial (astroglia and microglia) transcripts. The increase in glial transcripts likely indicates progressive activation of astrocytes and microglia, as observed previously in experimental [37–39] and human cerebral malaria [40–42]. Astrocytes form part of the neurovascular unit (NVU), interact with neurons and the vascular system [43], and thus respond to neuronal and vascular stress signals. The astroglia cell response is usually marked by increased expression of protein constituents of astrocyte intermediate filaments, including GFAP and NCAN [28,29]. We observed that the corresponding RNA from GFAP and NCAN in plasma EVs from cerebral malaria patients increased with disease progression. Although our data showing neuronal decline and increased gliosis is consistent with the trend observed in neurodegenerative disease progression[44], neurological impairment in cerebral malaria is usually reversible, except in the minority with severe disease, suggesting that gliosis in cerebral malaria indicates an early response to vascular injury or neuronal hypofunction such as synapse loss[45] and not overt neuronal death, except in extremely severe cases [34].

Taking our findings together, we propose the following: that reduced microcirculatory flow resulting from parasite sequestration in the brain[46,47] results suboptimal brain perfusion[48–50] and neuronal hypofunction (evidenced by falling neuronal transcript levels), which is associated with progressive increase in glial cell activity[43] (evidenced by a progressive increase in glial transcripts), and other vascular- (VEGFA-VEGFR2 signalling[51–57], platelet activation and coagulation[58]), and neuronal- (neurotrophin signalling[59], long-term potentiation[60] and glutamatergic signaling[61,62]) related adaptive processes during late-stages of cerebral malaria, which may turn maladaptive and pathological[60,63].

In conclusion, we show that the contents of circulating EVs can be used to study the brain in patients with cerebral malaria. We demonstrate that the molecular sequence of neurovascular events in cerebral malaria is accessible antemortem via EVs, despite the inaccessibility of neuronal tissue to direct sampling. This will allow a more complete study of the pathogenesis of the illness, identification of biomarkers to predict disease progression and design of therapeutic interventions.

Methods

Samples and design

The EV-RNAseq data was generated from 76 archived plasma samples from children with cerebral malaria who had been assessed for retinopathy and eight community-control adults without *P. falciparum* infection. Ethical approval of the study was provided by the Scientific Ethics Review Unit (SERU) of the Kenya Medical Research Institute (KEMRI) under the protocol KEMRI/SERU/3149. Written consents were provided by the parents or guardians of the children who donated the plasma samples. The subset of patients included in this study represented the whole cohort, as the proportion of CM-R^+ 30/76 (39%) and CM-R^- 46/76 (61%) were largely similar to those documented in the original studies

[21,22]. The sample size of the study was pragmatically determined based on available samples, clinical data, and resources.

Isolation of EVs from plasma and RNA extraction

Plasma was diluted in 13.5 ml of PBS and passed through a 0.22 µM filter. The filtrate was transferred into new ultracentrifuge tubes and spun at 150000 x g for 2 h at 4℃. The supernatant was discarded while the pellet was resuspended in 300 µL of PBS and treated with RNase A at 37 ℃ to digest non-vesicular RNA. After 15 minutes, the mixture was transferred to 13.5 ml ultracentrifuge tubes (Beckman). The tubes were filled using PBS and ultracentrifuged at 150000 x g for 2 h at 4 ℃. The final pellets were digested using 250 µl of RNA lysis buffer (Bioline) and kept at -80 ℃ until when required. RNA was isolated using the Isolate II RNA Min Kit (Bioline), following the manufacturer's instructions. Bead-assisted flow cytometry using antibodies to EV markers CD63 and CD9 was used to validate the EV isolation protocol.

Library preparation from plasma EV-RNA

The dUTP protocol developed by Chappell and others [64] was used to prepare the cDNA libraries for sequencing. Briefly, total EV-RNA is used to generate the first strand. Before second strand synthesis, the samples were cleaned using RNAcleanXP beads to remove traces of dNTPs. During the synthesis of the second strand, dTTP was replaced with dUTP. Double-stranded cDNA was then enzymatically shredded and ligated to NEXTflex adapters. The cDNA was treated with uracil glycosylase, which digests dUTPs to make the libraries strand-specific and amplified in 15 cycles to increase yield. Sequencing was done in two batches: 1 using the Hiseq 4000 genome analyser at the Wellcome Sanger Institute (WSI), UK and 2 using the NextSeq 500 genome analyser at the International Livestock Research Institute (ILRI), Kenya.

Normalisation of RNAseq data

RNAseq fastq files were quality-checked, and transcript read estimates were obtained by aligning the data to the human transcriptome using Kallisto [65]. The count data were normalised by gene length and sequencing depth, converted to counts per million (CPM) units, and used as input for all downstream analyses.

Deconvolution of EV-RNA data

Support vector regression was used to estimate the RNA fractions of solid tissue and brain cell-specific RNA. The solid tissue signature matrix used is publically available [24], while the brain cell signature matrix was constructed from the Darmanis brain cell data [66]. The blood-tissue matrix was generated by determining marker genes between solid tissues and blood using the Human Protein Atlas tissue RNAseq data [67]. The Seurat tool was used to select the markers to find the tissue-specific markers.

Estimation of cerebral malaria progression pseudotime

We used deep learning to estimate pseudotimes of the EV transcriptome samples. A pseudotime trajectory was inferred from the CPM data using PhenoPath [68] and fine-tuned using Slingshot [69]. PhenoPath is a tool that employs Bayesian statistics to model the latent expression of each sample. Harmonic regression models were fitted to determine the EV-RNAs altered as a function of the inferred disease pseudotime, and a nominal p-value < 0.05 was used as the cut-off for significance. Linear regression and ROC were used to compare pseudotime to retinopathy and other clinicopathological parameters, while Spearman's rank correlation was applied to determine association of brain cell EV-RNA fractions with disease progression pseduotime. The phaseogram of disease progression was constructed using ComplexHeatmap and subdivided into four clusters using kmeans [70]. The overlap between the four clusters and a published reference list of brain cell-specific markers [26,27] was tested using Fisher's exact test. KEGG and Wikipathway analysis were also performed using Fisher's exact test.

Declarations

Data availability

The EV-RNAseq is available from Gene Expression Omnibus (GEO) under the accession number GSE242856 (https://www.ncbi.nlm.nih.gov/geo/query/acc.cgi?acc=GSE242856). The following secure token can be used to review our data: gdodqoacptkbpcv. The HCC data was obtained from the GEO repository under the accession number GSE100207. The Darmanis single-cell RNAseq data is available from GEO under the accession number GSE67835. The solid tissue signature matrix was downloaded from https://github.com/HuangLab-Fudan/EV-origin/blob/master/Matrix_tissue.csv. The HPA tissue RNAseq data was downloaded from https://www.proteinatlas.org/download/normal_tissue.tsv.zip.

Code availability

No new software was generated in this study.

Acknowledgements

This work was supported by Wellcome Trust Awards: 209289/Z/17/Z (to AIA), 222323/Z/21/Z and 206194/Z/17/Z (to JCR) and 203077/Z/16/Z (a core Award to KEMRI-Wellcome Trust Research Programme). MK was supported by the Initiative to Develop African Research Leaders (IDeAL), part of DELTAS Africa Initiative [DEL-15-003]. For Open Access purposes, the author has applied a CC-BY public copyright licence to any author-accepted manuscript version arising from this submission. The funder had no role in study design, data collection and analysis, the decision to publish, or the writing of the manuscript.

Author Contributions

Conceptualisation: M.K, S.M, A.P, P.B, J.C.R, A.I.A

Methodology: M.K, S.M, P.B, J.C.R, A.I.A

Investigation: M.K, S.M, A.P, I.L.O, S.K, C.N, P.B, J.C.R, A.I.A

Visualisation: M.K, A.I.A

Funding acquisition: P.B, J.C.R, A.I.A

Project administration: P.B, J.C.R, A.I.A

Supervision: A.P, P.B, J.C.R, A.I.A

Writing – original draft: M.K, A.P, P.B, J.C.R, A.I.A

Writing – review & editing: M.K, S.M, A.P, I.L.O, S.K, C.N, P.B, J.C.R, A.I.A

Competing Interests

The authors declare that they have no competing interests.

References

1. Marsh, K. *et al.* Indicators of life-threatening malaria in African children. *N Engl J Med* **332**, 1399-1404 (1995).
2. White, N. J. & Ho, M. The pathophysiology of malaria. *Adv Parasitol* **31**, 83-173 (1992). https://doi.org:10.1016/s0065-308x(08)60021-4
3. Newton, C. R., Taylor, T. E. & Whitten, R. O. Pathophysiology of fatal falciparum malaria in African children. *Am J Trop Med Hyg* **58**, 673-683 (1998). https://doi.org:10.4269/ajtmh.1998.58.673
4. Taylor, T. E. *et al.* Differentiating the pathologies of cerebral malaria by postmortem parasite counts. *Nature Medicine* **10**, 143-145 (2004). https://doi.org:10.1038/nm986
5. MacCormick, I. J. *et al.* Cerebral malaria in children: using the retina to study the brain. *Brain : a journal of neurology* **137**, 2119-2142 (2014). https://doi.org:10.1093/brain/awu001
6. Barrera, V. *et al.* Severity of retinopathy parallels the degree of parasite sequestration in the eyes and brains of malawian children with fatal cerebral malaria. *J Infect Dis* **211**, 1977-1986 (2015). https://doi.org:10.1093/infdis/jiu592
7. Greiner, J. *et al.* Correlation of hemorrhage, axonal damage, and blood-tissue barrier disruption in brain and retina of Malawian children with fatal cerebral malaria. *Front Cell Infect Microbiol* **5**, 18 (2015). https://doi.org:10.3389/fcimb.2015.00018
8. Harding, S. P. *et al.* Classifying and grading retinal signs in severe malaria. *Trop Doct* **36 Suppl 1**, 1-13 (2006). https://doi.org:10.1258/004947506776315781
9. Beare, N. A. *et al.* Prognostic significance and course of retinopathy in children with severe malaria. *Arch Ophthalmol* **122**, 1141-1147 (2004). https://doi.org:10.1001/archopht.122.8.1141 122/8/1141 [pii]

10. Schémann, J. F. *et al.* Ocular lesions associated with malaria in children in Mali. *Am J Trop Med Hyg* **67**, 61-63 (2002). https://doi.org:10.4269/ajtmh.2002.67.61
11. Essuman, V. A. *et al.* Retinopathy in severe malaria in Ghanaian children--overlap between fundus changes in cerebral and non-cerebral malaria. *Malar J* **9**, 232 (2010). https://doi.org:1475-2875-9-232 [pii] 10.1186/1475-2875-9-232
12. Abu Sayeed, A. *et al.* Malarial retinopathy in Bangladeshi adults. *Am J Trop Med Hyg* **84**, 141-147 (2011). https://doi.org:10.4269/ajtmh.2011.10-0205
13. Beare, N. A., Taylor, T. E., Harding, S. P., Lewallen, S. & Molyneux, M. E. Malarial retinopathy: a newly established diagnostic sign in severe malaria. *Am J Trop Med Hyg* **75**, 790-797 (2006). https://doi.org:75/5/790 [pii]
14. Soliz, P. *et al.* Comparison of the effectiveness of three retinal camera technologies for malarial retinopathy detection in Malawi. *Proc SPIE Int Soc Opt Eng* **9693** (2016). https://doi.org:10.1117/12.2213282
15. Raposo, G. & Stoorvogel, W. Extracellular vesicles: exosomes, microvesicles, and friends. *J Cell Biol* **200**, 373-383 (2013). https://doi.org:10.1083/jcb.201211138
16. Hallal, S. *et al.* The emerging clinical potential of circulating extracellular vesicles for non-invasive glioma diagnosis and disease monitoring. *Brain Tumor Pathol* **36**, 29-39 (2019). https://doi.org:10.1007/s10014-019-00335-0
17. Rennert, R. C., Hochberg, F. H. & Carter, B. S. ExRNA in Biofluids as Biomarkers for Brain Tumors. *Cell Mol Neurobiol* **36**, 353-360 (2016). https://doi.org:10.1007/s10571-015-0284-5
18. Mukherjee, S. *et al.* Molecular estimation of neurodegeneration pseudotime in older brains. *Nature Communications* **11**, 5781 (2020). https://doi.org:10.1038/s41467-020-19622-y
19. Huang, K. *et al.* Inferring evolutionary trajectories from cross-sectional transcriptomic data to mirror lung adenocarcinoma progression. *PLoS Comput Biol* **19**, e1011122 (2023). https://doi.org:10.1371/journal.pcbi.1011122
20. Magwene, P. M., Lizardi, P. & Kim, J. Reconstructing the temporal ordering of biological samples using microarray data. *Bioinformatics* **19**, 842-850 (2003). https://doi.org:10.1093/bioinformatics/btg081
21. Abdi, A. I. *et al.* Differential Plasmodium falciparum surface antigen expression among children with Malarial Retinopathy. *Scientific Reports* **5**, 18034 (2015). https://doi.org:10.1038/srep18034
22. Kariuki, S. M. *et al.* Value of Plasmodium falciparum Histidine-Rich Protein 2 Level and Malaria Retinopathy in Distinguishing Cerebral Malaria From Other Acute Encephalopathies in Kenyan Children. *The Journal of Infectious Diseases* **209**, 600-609 (2013). https://doi.org:10.1093/infdis/jit500
23. Cortes, C. & Vapnik, V. Support-vector networks. *Machine Learning* **20**, 273-297 (1995). https://doi.org:10.1007/BF00994018
24. Li, Y. *et al.* EV-origin: Enumerating the tissue-cellular origin of circulating extracellular vesicles using exLR profile. *Comput Struct Biotechnol J* **18**, 2851-2859 (2020).

https://doi.org:10.1016/j.csbj.2020.10.002

25. Li, S. *et al.* exoRBase: a database of circRNA, lncRNA and mRNA in human blood exosomes. *Nucleic Acids Research* **46**, D106-D112 (2017). https://doi.org:10.1093/nar/gkx891
26. Franzén, O., Gan, L. M. & Björkegren, J. L. M. PanglaoDB: a web server for exploration of mouse and human single-cell RNA sequencing data. *Database (Oxford)* **2019** (2019). https://doi.org:10.1093/database/baz046
27. McKenzie, A. T. *et al.* Brain Cell Type Specific Gene Expression and Co-expression Network Architectures. *Scientific Reports* **8**, 8868 (2018). https://doi.org:10.1038/s41598-018-27293-5
28. Asher, R. A. *et al.* Neurocan Is Upregulated in Injured Brain and in Cytokine-Treated Astrocytes. *The Journal of Neuroscience* **20**, 2427-2438 (2000). https://doi.org:10.1523/jneurosci.20-07-02427.2000
29. Yang, Z. & Wang, K. K. Glial fibrillary acidic protein: from intermediate filament assembly and gliosis to neurobiomarker. *Trends Neurosci* **38**, 364-374 (2015). https://doi.org:10.1016/j.tins.2015.04.003
30. Verkman, A. S., Binder, D. K., Bloch, O., Auguste, K. & Papadopoulos, M. C. Three distinct roles of aquaporin-4 in brain function revealed by knockout mice. *Biochim Biophys Acta* **1758**, 1085-1093 (2006). https://doi.org:10.1016/j.bbamem.2006.02.018
31. Kanehisa, M., Sato, Y., Kawashima, M., Furumichi, M. & Tanabe, M. KEGG as a reference resource for gene and protein annotation. *Nucleic Acids Research* **44**, D457-D462 (2015). https://doi.org:10.1093/nar/gkv1070
32. Kutmon, M. *et al.* WikiPathways: capturing the full diversity of pathway knowledge. *Nucleic Acids Res* **44**, D488-494 (2016). https://doi.org:10.1093/nar/gkv1024
33. English, M. *et al.* Assessment of inpatient paediatric care in first referral level hospitals in 13 districts in Kenya. *Lancet* **363**, 1948-1953 (2004). https://doi.org:10.1016/S0140-6736(04)16408-8
34. Idro, R., Carter, J. A., Fegan, G., Neville, B. G. & Newton, C. R. Risk factors for persisting neurological and cognitive impairments following cerebral malaria. *Arch Dis Child* **91**, 142-148 (2006). https://doi.org:10.1136/adc.2005.077784
35. Idro, R., Marsh, K., John, C. C. & Newton, C. R. Cerebral malaria: mechanisms of brain injury and strategies for improved neurocognitive outcome. *Pediatr Res* **68**, 267-274 (2010). https://doi.org:10.1203/PDR.0b013e3181eee738
36. Small, D. S. *et al.* Evidence from a natural experiment that malaria parasitemia is pathogenic in retinopathy-negative cerebral malaria. *Elife* **6** (2017). https://doi.org:10.7554/eLife.23699
37. Medana, I. M., Chan-Ling, T. & Hunt, N. H. Redistribution and degeneration of retinal astrocytes in experimental murine cerebral malaria: relationship to disruption of the blood-retinal barrier. *Glia* **16**, 51-64 (1996). https://doi.org:10.1002/(sici)1098-1136(199601)16:1<51::Aid-glia6>3.0.Co;2-e
38. Medana, I. M., Hunt, N. H. & Chan-Ling, T. Early activation of microglia in the pathogenesis of fatal murine cerebral malaria. *Glia* **19**, 91-103 (1997). https://doi.org:10.1002/(sici)1098-1136(199702)19:2<91::aid-glia1>3.0.co;2-c

39. Ma, N., Madigan, M. C., Chan-Ling, T. & Hunt, N. H. Compromised blood-nerve barrier, astrogliosis, and myelin disruption in optic nerves during fatal murine cerebral malaria. *Glia* **19**, 135-151 (1997). https://doi.org:10.1002/(sici)1098-1136(199702)19:2<135::aid-glia5>3.0.co;2-#
40. Janota, I. & Doshi, B. Cerebral malaria in the United Kingdom. *J Clin Pathol* **32**, 769-772 (1979). https://doi.org:10.1136/jcp.32.8.769
41. Medana, I. M. *et al.* Axonal injury in cerebral malaria. *Am J Pathol* **160**, 655-666 (2002). https://doi.org:10.1016/s0002-9440(10)64885-7
42. Schluesener, H. J., Kremsner, P. G. & Meyermann, R. Widespread expression of MRP8 and MRP14 in human cerebral malaria by microglial cells. *Acta Neuropathol* **96**, 575-580 (1998). https://doi.org:10.1007/s004010050938
43. Sofroniew, M. V. Astrocyte barriers to neurotoxic inflammation. *Nat Rev Neurosci* **16**, 249-263 (2015). https://doi.org:10.1038/nrn3898
44. Mukherjee, S. *et al.* Molecular estimation of neurodegeneration pseudotime in older brains. *Nat Commun* **11**, 5781 (2020). https://doi.org:10.1038/s41467-020-19622-y
45. Escartin, C. *et al.* Reactive astrocyte nomenclature, definitions, and future directions. *Nat Neurosci* **24**, 312-325 (2021). https://doi.org:10.1038/s41593-020-00783-4
46. Silamut, K. *et al.* A quantitative analysis of the microvascular sequestration of malaria parasites in the human brain. *Am J Pathol* **155**, 395-410 (1999). https://doi.org:S0002-9440(10)65136-X [pii] 10.1016/S0002-9440(10)65136-X
47. Taylor, T. E. *et al.* Differentiating the pathologies of cerebral malaria by postmortem parasite counts. *Nat Med* **10**, 143-145 (2004). https://doi.org:10.1038/nm986 nm986 [pii]
48. White, N. J., Turner, G. D., Day, N. P. & Dondorp, A. M. Lethal malaria: Marchiafava and Bignami were right. *J Infect Dis* **208**, 192-198 (2013). https://doi.org:10.1093/infdis/jit116
49. Day, N. P. *et al.* The pathophysiologic and prognostic significance of acidosis in severe adult malaria. *Crit Care Med* **28**, 1833-1840 (2000).
50. Warrell, D. A. *et al.* Cerebral anaerobic glycolysis and reduced cerebral oxygen transport in human cerebral malaria. *Lancet* **2**, 534-538 (1988). https://doi.org:10.1016/s0140-6736(88)92658-x
51. Conroy, A. L. *et al.* Endothelium-based biomarkers are associated with cerebral malaria in Malawian children: a retrospective case-control study. *PLoS One* **5**, e15291 (2010). https://doi.org:10.1371/journal.pone.0015291
52. Lan, G. *et al.* Astrocytic VEGFA: An essential mediator in blood-brain-barrier disruption in Parkinson's disease. *Glia* **70**, 337-353 (2022). https://doi.org:10.1002/glia.24109
53. Manukjan, N. *et al.* Hypoxic oligodendrocyte precursor cell-derived VEGFA is associated with blood-brain barrier impairment. *Acta Neuropathol Commun* **11**, 128 (2023). https://doi.org:10.1186/s40478-023-01627-5
54. Shweiki, D., Itin, A., Soffer, D. & Keshet, E. Vascular endothelial growth factor induced by hypoxia may mediate hypoxia-initiated angiogenesis. *Nature* **359**, 843-845 (1992).

https://doi.org:10.1038/359843a0

55. Argaw, A. T., Gurfein, B. T., Zhang, Y., Zameer, A. & John, G. R. VEGF-mediated disruption of endothelial CLN-5 promotes blood-brain barrier breakdown. *Proc Natl Acad Sci U S A* **106**, 1977-1982 (2009). https://doi.org:10.1073/pnas.0808698106
56. Smith, R. O. *et al.* Vascular permeability in retinopathy is regulated by VEGFR2 Y949 signaling to VE-cadherin. *Elife* **9** (2020). https://doi.org:10.7554/eLife.54056
57. Pérez-Gutiérrez, L. & Ferrara, N. Biology and therapeutic targeting of vascular endothelial growth factor A. *Nat Rev Mol Cell Biol* (2023). https://doi.org:10.1038/s41580-023-00631-w
58. Gramaglia, I. *et al.* Platelets activate a pathogenic response to blood-stage Plasmodium infection but not a protective immune response. *Blood* **129**, 1669-1679 (2017). https://doi.org:10.1182/blood-2016-08-733519
59. Reichardt, L. F. Neurotrophin-regulated signalling pathways. *Philos Trans R Soc Lond B Biol Sci* **361**, 1545-1564 (2006). https://doi.org:10.1098/rstb.2006.1894
60. Weiss, S., Mori, F., Rossi, S. & Centonze, D. Disability in multiple sclerosis: when synaptic long-term potentiation fails. *Neurosci Biobehav Rev* **43**, 88-99 (2014). https://doi.org:10.1016/j.neubiorev.2014.03.023
61. Franchini, L., Carrano, N., Di Luca, M. & Gardoni, F. Synaptic GluN2A-Containing NMDA Receptors: From Physiology to Pathological Synaptic Plasticity. *Int J Mol Sci* **21** (2020). https://doi.org:10.3390/ijms21041538
62. Gataullina, S. *et al.* GluN2C selective inhibition is a target to develop new antiepileptic compounds. *Epilepsia* **63**, 2911-2924 (2022). https://doi.org:10.1111/epi.17396
63. Meizlish, M. L., Franklin, R. A., Zhou, X. & Medzhitov, R. Tissue Homeostasis and Inflammation. *Annu Rev Immunol* **39**, 557-581 (2021). https://doi.org:10.1146/annurev-immunol-061020-053734
64. Chappell, L. *et al.* Refining the transcriptome of the human malaria parasite Plasmodium falciparum using amplification-free RNA-seq. *BMC Genomics* **21**, 395 (2020). https://doi.org:10.1186/s12864-020-06787-5
65. Bray, N. L., Pimentel, H., Melsted, P. & Pachter, L. Near-optimal probabilistic RNA-seq quantification. *Nature Biotechnology* **34**, 525-527 (2016). https://doi.org:10.1038/nbt.3519
66. Darmanis, S. *et al.* A survey of human brain transcriptome diversity at the single cell level. *Proc Natl Acad Sci U S A* **112**, 7285-7290 (2015). https://doi.org:10.1073/pnas.1507125112
67. Thul, P. J. & Lindskog, C. The human protein atlas: A spatial map of the human proteome. *Protein Sci* **27**, 233-244 (2018). https://doi.org:10.1002/pro.3307
68. Campbell, K. R. & Yau, C. Uncovering pseudotemporal trajectories with covariates from single cell and bulk expression data. *Nat Commun* **9**, 2442 (2018). https://doi.org:10.1038/s41467-018-04696-6
69. Street, K. *et al.* Slingshot: cell lineage and pseudotime inference for single-cell transcriptomics. *BMC Genomics* **19**, 477 (2018). https://doi.org:10.1186/s12864-018-4772-0

70. Gu, Z., Eils, R. & Schlesner, M. Complex heatmaps reveal patterns and correlations in multidimensional genomic data. *Bioinformatics* **32**, 2847-2849 (2016). https://doi.org:10.1093/bioinformatics/btw313

Supplementary Files

Supplementary Data Files are not available with this version

Figures

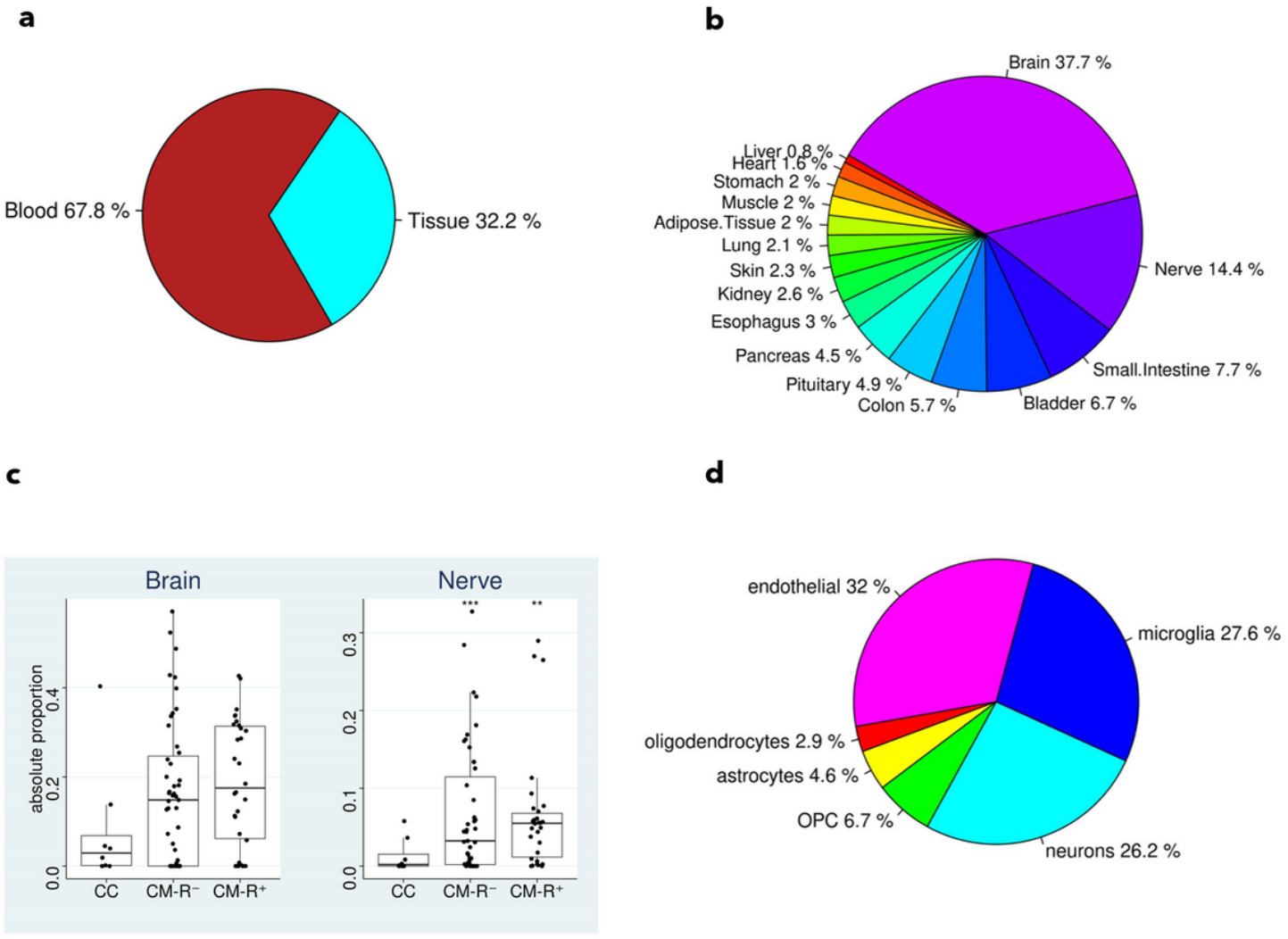

Figure 1

Brain-derived RNAs are enriched in circulating EVs

a The relative comparison of blood and solid tissue RNA fractions in plasma EVs from cerebral malaria patients. **b** The relative distributions of solid tissue fractions of circulating EVs in cerebral malaria. **c** The estimated absolute proportion of RNA expressed by brain and nerves is higher in retinopathy positive

(CM-R$^+$) and negative (CM-R$^-$) cerebral malaria compared to community controls (CC). **d** Brain cell relative fractions estimated from the plasma EV-RNA data.

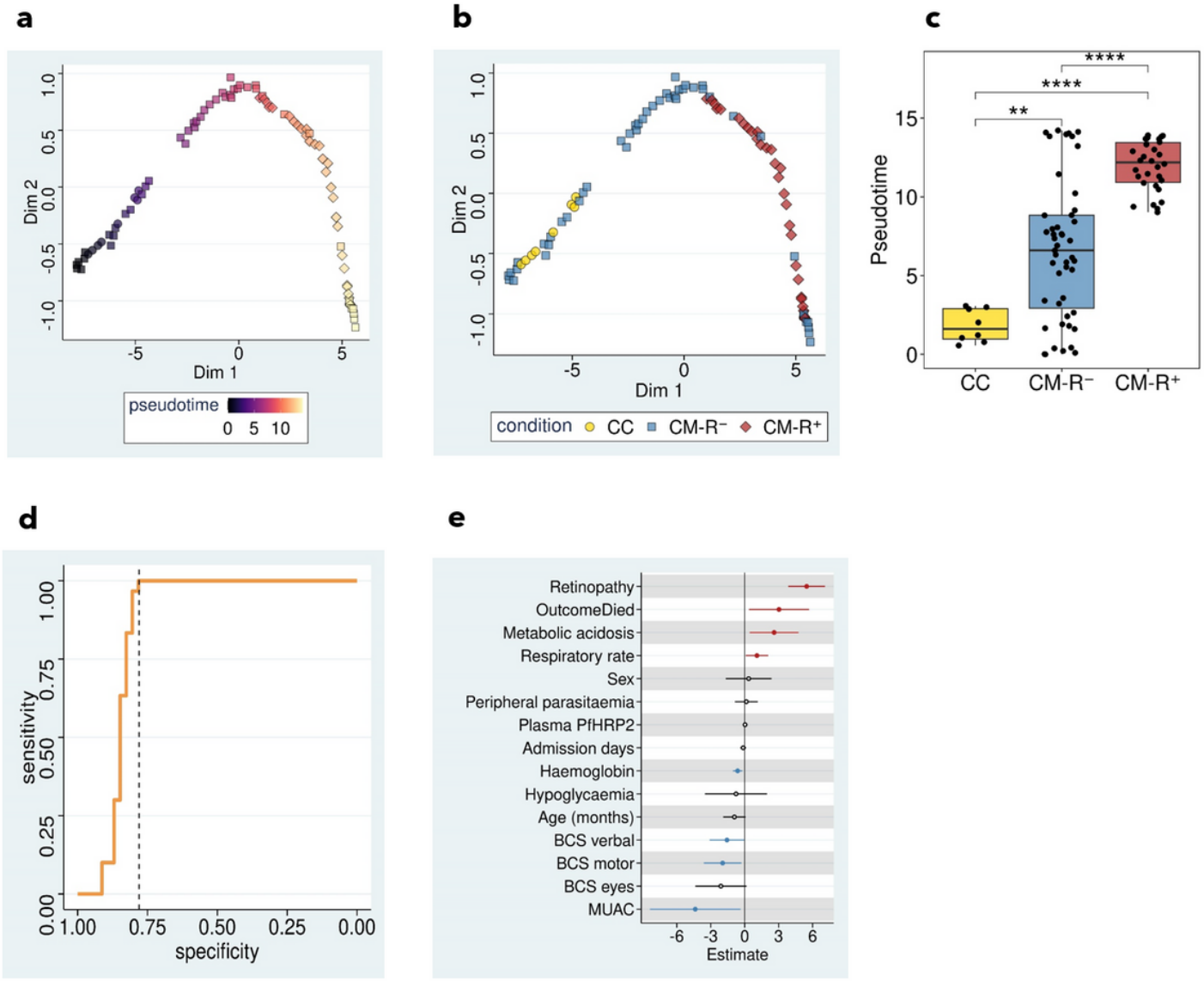

Figure 2

Manifold learning infers disease stage from plasma-EV transcriptomes

a EV-RNA samples coloured by disease progression pseudotime. The scatter plot shows that cerebral malaria evolves in a single trajectory **b** EV-RNA samples coloured by retinopathy status depicting that late stage pseudotime are enriched for the CM-R+ sample set. **c** Boxplots comparing disease pseudotime between CC, CM-R- and CM-R+. Inferred disease stage is significantly more advanced in CM-R+ than CM-R-. **d** A Forest plot showing results of linear regression comparing retinopathy and clinical parameters. Red shows positive correlations, black non-significant correlations, and blue negative correlations. The estimated pseudotime is concordant with known clinical parameters. **e** ROC curve showing that

retinopathy is 100% sensitive and 78% specific that cerebral malaria has progressed to late stage pseudotime.

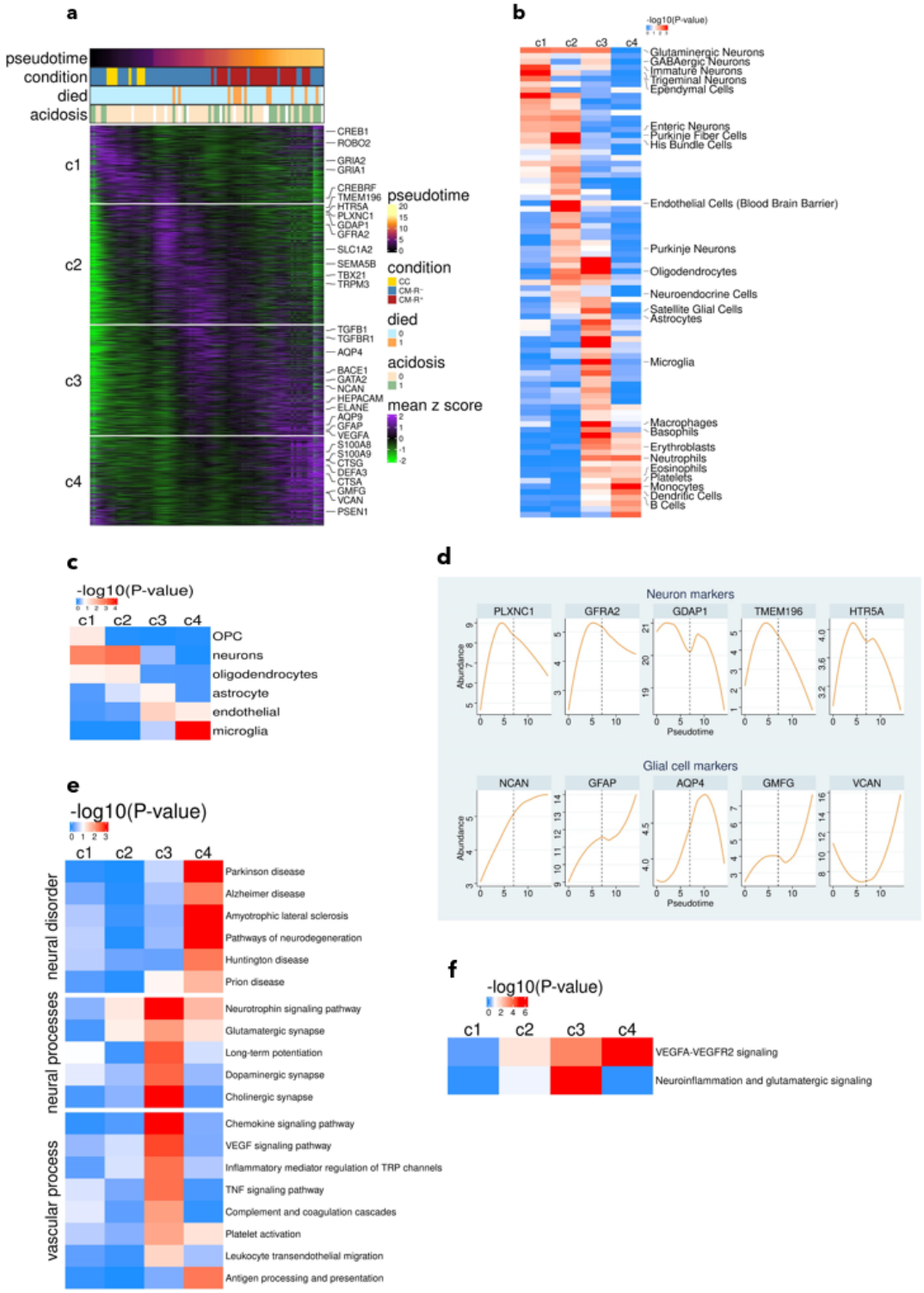

Figure 3

Brain-derived plasma EV-RNA varies over pseudotime

a Phaseogram showing variation of plasma EV-RNA as a function of disease progression pseudotime. The transcripts are clustered along pseudotime revealing four clusters, c1 to c4. **b** Enrichment analysis using PanglaoDB cell markers shows that early pseudotime clusters (c1 and c2) are enriched for neuronal markers while late pseudotime clusters are enriched for glial (oligodendrocyte, astrocyte and microglia) and immune cells. **c** Enrichment analysis using Darmanis brain cell markers also shows that cerebral malaria is characterized by neuronal loss and increased glial gene expression. **d** Representative EV-RNA profiles of neuronal and glial cell markers. **e** KEGG enrichment analysis results showing that cluster 3 is enriched for transcripts belonging to vascular processes and neural functions while cluster 4 is enriched for transcripts linked to pathways of neurodegeneration. **f** Wikipathway enrichment analysis results showing that genes involved in VEGFA-VEGFR2 signalling and neuroinflammation and glutamatergic signalling belonged to late-stage clusters

Supplementary Files

This is a list of supplementary files associated with this preprint. Click to download.

- BrainEVMSSupplementaryfiguresubmitted.pdf